JOURNAL OF MATERIALS SCIENCE 28 (1993) 6676–6682

Mechanical properties of phosphate glass-ceramic–316 L stainless steel composites

F. PERNOT, R. ROGIER
Laboratoire de Science des Matériaux Vitreux – C.N.R.S., U.R.A. 1119, U.S.T.L. Place E. Bataillon, 34095 Montpellier Cédex 05, France

Thermal, elastic and mechanical properties of phosphate glass-ceramic–316 L stainless steel particulate composites, prepared by flash-pressing, have been measured. Results have then been explained using various theoretical models. It is shown that particles partly shrink away from the matrix on cooling; this is due both to the slight thermal mismatch between glass-ceramic matrix and 316 L stainless steel particles and to poor bonding between both phases. This small partial shrinkage could explain both the fracture characteristics and the fair agreement between theoretical and experimental values of elastic moduli.

1. Introduction

During the last four decades there has been an increasing demand for high-performance materials for use in a diverse range of applications from aerospace and military to biomedical [1, 2]. In this last field, glass-ceramic–metal particulate composites have been synthesized previously from powdered mixtures of a calcium alumino-phosphate glass (CAP) with various biocompatible metals or alloys (titanium, 316 L stainless steel, cobalt–chromium 788 alloy) commonly used in orthopaedics. They have been proposed to act as thermal and elastic graded seals between various dense metal cores of prostheses and a porous phosphate glass-ceramic coating [3, 4].

Detailed studies on thermal, elastic behaviour and fracture mechanics of CAP glass-ceramic–titanium and CAP glass-ceramic–cobalt–chromium composites have been also carried out previously [5, 6]. This paper deals with basic understanding on thermal and deformation behaviour, strength and toughness of phosphate glass-ceramic–316 L stainless steel particulate composites.

2. Experimental procedure

2.1. Base products and preparation of composites

The parent calcium alumino-phosphate glass (CAP) is composed of 69.0% P_2O_5, 22.7% CaO, 8.3% Al_2O_3 in weight ratio. It was prepared from a mixture of calcium bis-dihydrogen phosphate and hydrated aluminium orthophosphate, which was melted in a Pt–10% Rh crucible at 1300 °C for 2 h, then crushed into a powder with a particle size lower than 50 μm. 316 L stainless steel is a commercial product ("Baudier-Poudmet"); it has the following composition for the more important alloying elements: 17.3% Cr, 12.9% Ni, 2.2% Mo, 0.8% Si, 0.3% Mn, < 0.03% C, balance iron, in weight ratio. Particles, which are not necessarily spherical have a size below 60 μm with an average "equivalent spherical diameter" [7] of 25 μm. Properties of the parent glass, glass-ceramic and 316 L stainless steel are summarized in Table I.

Six mixtures of CAP glass with increasing volume fractions (from 3.5%–50%) of 316 L stainless steel particles were vacuum-hot-pressed into composite discs of about 38 mm diameter and 5 mm thickness; the "flash pressing" method was used [3, 8]. Pressure was removed as soon as the samples were totally sintered. They were then kept at about 700 °C for 1 h to obtain total ceramization of the matrix. Two or three discs of each composition were thus prepared.

2.2. Methods of measurement

2.2.1. Thermal properties

Linear thermal expansion was measured with a differential dilatometer (D.I. 10-2, Adamel-Lhomargy) using vitreous silica as a reference material. Measurements were made from room temperature to 750 °C, at a linear heating rate of 3 °C min^{-1}.

The relative expansion at each temperature and the average linear thermal expansion coefficients were deduced from the recorded curves [3].

2.2.2. Elastic properties

Elastic properties were determined using a dynamic method based on the magnetostrictive effect [3]. The specimen resonators may be chosen either as square shaped bars or discs. Only Young's modulus can be measured using bars; discs are used for the determination of both Young's modulus and Poisson's ratio. The knowledge of two elastic constants allows calculation of the others [3, 9].

2.2.3. Mechanical properties

Flexural strength, σ_R, and fracture toughness, K_{IC}, were measured on square-shaped bars, by three-point bend tests.

0022–2461

Fracture strength determination was carried out on 1.5 mm × 3 mm × 15 mm specimens, with a 12 mm span. The testing machine (Instron 1196) operated at a loading rate of 0.1 mm min^{-1}. All measurements were made in air at room temperature. For each composite, seven to sixteen specimens were fractured.

Toughness values were determined using 2 mm × 4 mm × 24 mm single-edge notched bend specimens, which were fractured over a 16 mm span. A notch as thin as possible of 1.3 mm depth was machined at the midpoint of one 24 mm edge of each specimen. Samples (two to nine for each composite) were tested at a crosshead speed of 0.05 mm min^{-1}. All measurements were performed in air at room temperature. Fracture toughness was calculated from specimen dimensions, notch depth and fracture load [3, 10].

The knowledge of E, K_{IC} and σ_R allows calculation of other mechanical characteristics: critical flaw size (the size of the defect from which the fracture starts), a_c; fracture energy, Γ [11, 12].

3. Results and discussion

3.1. Thermal properties

As in titanium and cobalt–chromium composite materials [5, 6], the expansion curves of 316 L stainless steel composites (Fig. 1) show a shoulder between 100 and 200 °C, which is due to $\alpha \rightleftharpoons \beta$ transformation of $AlPO_4$ cristobalite form [13, 14] in the glass-ceramic matrix. Sometimes, other features occur at higher temperatures; those which are observed close to 500 °C could be due to a residual vitreous phase in the matrix.

The average linear thermal expansion coefficients have been calculated between 20 and 500 °C (α_{20-500}), 20 and 700 °C (α_{20-700}), respectively. These experimental data have been compared with various models, which predict theoretical evolutions of α as a function of 316 L volume fraction, c_p, and in terms of the thermal and elastic properties of the components [15–17] (Fig. 2).

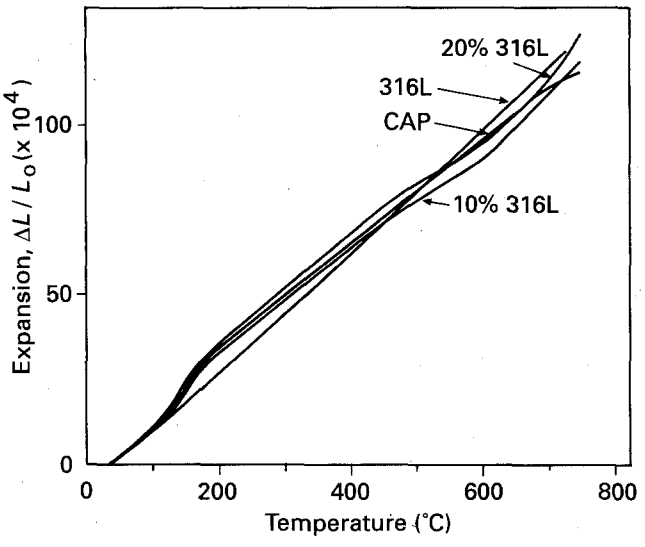

Figure 1 Linear thermal expansion of CAP glass-ceramic–316 L stainless steel composites.

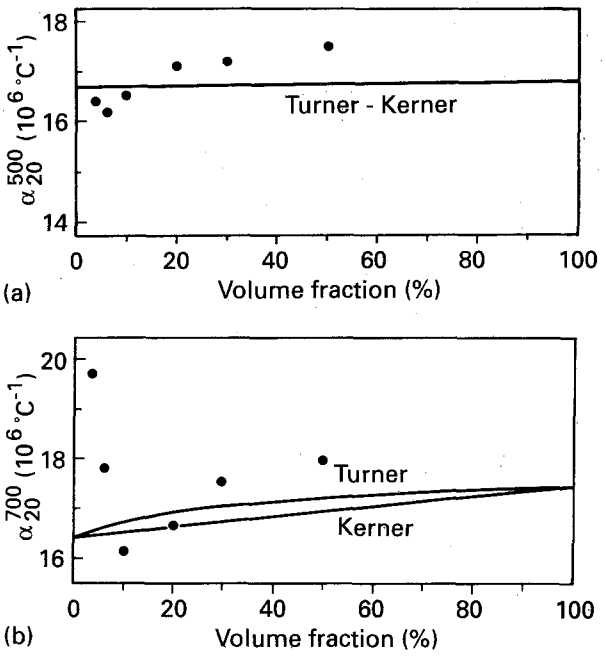

Figure 2 Theoretical and experimental average linear thermal expansion coefficients of CAP glass-ceramic–316 L stainless steel composites: (a) α_{20-500}; (b) α_{20-700}.

In the temperature range 20–500 °C, because α_{316L} (16.8×10^{-6} °C^{-1}) is close to α_{CAP} (16.7×10^{-6} °C^{-1}) (Table I), Kerner and Turner models [15, 17] give the same straight line; the experimental values of coefficients α_{20-500} are close to this line and do not show significant evolution as a function of metal content (Fig. 2a).

In the range 20–700 °C, α_{316L} (17.4×10^{-6} °C^{-1}) is a little higher than α_{CAP} (16.4×10^{-6} °C^{-1}) (Table I). As a result, Kerner and Turner curves [15, 17] are slightly different. Values of coefficients α_{20-700}, which are often disturbed by the features at high temperature, usually lie above the last curve (Fig. 2b).

3.2. Elastic properties

Young's modulus increases with the volume fraction, c_p, of 316 L stainless steel particles. The experimental results (Table II) have also been compared with values given by various models. These expressions predict theoretical evolution of Young's modulus of composites as a function of volume fraction of the second phase and from the elastic properties of individual components [17–21]. Most of them assume that strains and stresses are totally transferred from one phase to the other, which requires both a close contact between matrix and particles and no microcracking of materials. They have then representative curves lying within two limits: the upper bound, Voigt model [19] and the lower bound, Reuss model [20].

For most composites (from 6–50 vol % 316 L), experimental values fall just above Reuss's lower bound, but below other theoretical curves (Fig. 3). If it is assumed that theoretical Young's modulus, E_0, corresponds to the average between upper and lower bound of Hashin and Shtrikman's model [21], then,

TABLE I Properties of materials for the preparation of CAP glass-ceramic–316 L stainless steel composites

Properties		CAP glass	CAP glass-ceramic	316 L stainless steel
Density ($g\,cm^{-3}$)		2.64	2.65	7.95
Average linear expansion	α_{20-500}	9.3	16.7	16.8
coefficients ($10^6\,°C^{-1}$)	α_{20-700}	–	16.4	17.4
Young's modulus (GPa)		64	68	193
Poisson's ratio		0.256	0.180	0.30
Fracture stress (MPa)		53.9	146.7	520
				$\sigma_Y = 284$
Fracture toughness ($MPa\,m^{1/2}$)		0.78	2.22	–
Average radius of particles (μm)		$\leqslant$ 50	–	12.5

TABLE II Elastic and mechanical properties of CAP glass-ceramic–316 L stainless steel composites

316 L fraction (vol %)	Young's modulus (GPa)	Poisson's ratio	Fracture stress (MPa)	Fracture toughness ($MPa\,m^{1/2}$)	Critical flaw size, $2a_c$ (μm)		Mean free path (μm)
					Griffith flaw	Penny-shaped crack	
0	68	0.180	146.7	2.22	120	290	–
3.5	72	0.194	144.4	2.325	136	326	460
6	72	0.193	139.0	2.03	110	264	150
10	74	0.196	126.0	2.05	140	336	150
20	79	0.203	124.0	2.08	148	356	67
30	88	0.218	124.4	2.16	158	379	39
50	102	0.234	126.5	2.28	160	384	17
316 L	193	0.300	520	–	–	–	–

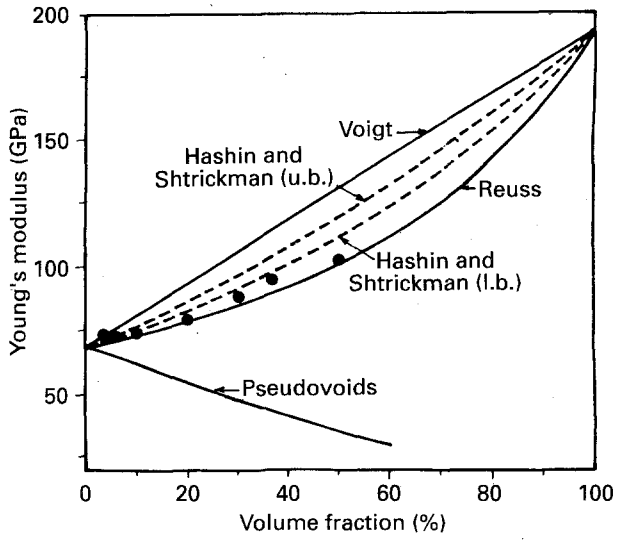

Figure 3 Theoretical and experimental Young's modulus of CAP glass-ceramic–316 L stainless steel composites.

for these 6%–50% composites, one or both conditions noticed above could not be totally fulfilled. Consequently, the following discussions will mainly concern the behaviour of these composites.

As the body cools from ceramization (700 °C) to room temperature (20 °C), because the coefficient of thermal expansion of the matrix is slightly lower than that of 316 L stainless steel (Table I), a residual stress field could be developed within and around particles, depending on the bonding characteristics of the glass-ceramic–316 L interface. If particles are well bonded to the matrix, each of them, assumed as spherical, is subjected to a uniform hydrostatic pressure, which can be estimated by [22, 23]

$$P_0 = \Delta\alpha\,\Delta T \Big/ \left(\frac{1+\nu_m}{2E_m} + \frac{1-2\nu_p}{E_p}\right) \quad (1)$$

$\Delta\alpha = \alpha_m - \alpha_p$; ΔT is the difference between ceramization and room temperature; ν_m, ν_p are Poisson's ratio of matrix and particles, respectively; E_m, E_p are Young's modulus of matrix and particles, respectively.

Substituting reported values of Table I into Equation 1, $P_0 = -63$ MPa. This pressure induces radial, σ_{rr}, and tangential, $\sigma_{\theta\theta}$ stresses in the matrix [23]

$$-\sigma_{rr} = 2\,\sigma_{\theta\theta} = P_0\left(\frac{R}{r}\right)^3 \quad (2)$$

where R is the radius of the particle and r the distance from the centre of the particle.

The radial tensile stress outside the particles, if sufficiently high, can initiate circumferencial cracks away from the particle–matrix interfaces [23–26]. This microcracking occurs only when particles reach a critical size, R_c, which can be estimated by Davidge and Green's equation [23]

$$R_c = 4\Gamma_m\left[P_0^2\left(\frac{1+\nu_m}{2E_m} + \frac{1-2\nu_p}{E_p}\right)\right]^{-1} \quad (3)$$

where Γ_m is the fracture energy of the matrix.

Substituting reported values in Equation 3 gives, for the critical radius, $R_c = 3300\ \mu m$ (3.3 mm). This is much higher than the average radius of 316 L stainless steel particles (12.5 μm). The occurrence of a circumferential microcracking in glass-ceramic–316 L stainless steel composites is totally unrealistic; their weakening is more probably due to a lack of bonding between matrix and 316 L stainless steel.

If particles are not bonded, whatever their size, they spontaneously shrink away from the matrix on cooling, as was shown previously in a borosilicate glass–nickel system [27]. However, in such a "true pseudo-porous" system, elastic moduli continuously decrease as increasing particles (i.e. "pseudovoids") volume fraction [28] (Fig. 3). It must, therefore, be concluded that 316 L stainless steel particles still partly contribute to the load-bearing ability of materials.

This can be explained by various mechanisms: (1) thermal mismatch is low, so that the lack of bonding between matrix and 316 L only produces a small shrinkage of particles; (2) the shrinkage is not necessarily homogeneous because most particles are not spherical; (3) if they are slightly oxidized, a partial bond could be obtained with the matrix during hot-pressing [29–31]. Because of these factors, it is not sure that particles are totally shrunk away from matrix after cooling.

This seems to be confirmed by scanning electron micrographs (Fig. 4), which show that most particles are surrounded by a thin void space, with a part of their surface still bonded to the matrix.

An expression for Young's modulus of composites containing partly debonded particles can then be obtained approximately assuming that: (1) particles are spherical (as already assumed using Equation 1 [22]); (2) departure between theoretical and experimental Young's modulus is due to thin void spaces, which are then considered as "spherical segment-shaped flaws" (Fig. 5); (3) the radius, R, of particles is large with respect to the size, a, of the flaws, which can then be considered as penny-shaped cracks.

With such hypotheses, convenient expression of Young's modulus for a random array of penny-shaped cracks, radius a, can be used [32, 33]

$$E = E_0\left[1 + \frac{16}{9} N_m a^3\right]^{-1} \quad (4)$$

where E_0 is Young's modulus of the uncracked material (i.e. theoretical Young's modulus assumed as being equal to the average between upper and lower bound of Hashin and Shtrikmans model [21]), and N_m is the microcrack density.

Because all particles are partly debonded, then N_m is equal to the number of particles, N_p, per unit volume and can be estimated from the formula for a random dispersion of equally sized spheres, radius R [33]

$$N_m = N_p = \frac{3 c_p}{4\pi R^3} \quad (5)$$

where c_p is the volume fraction, of 316 L particles.

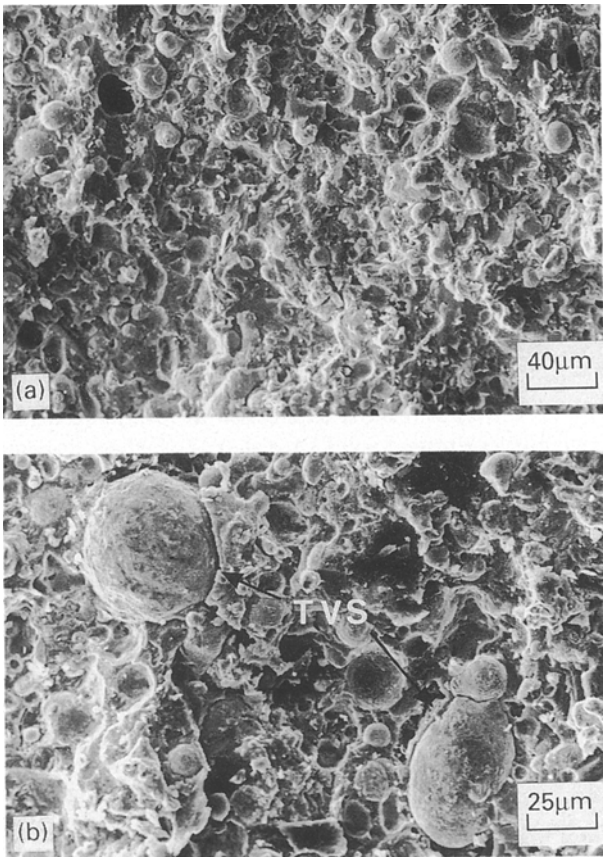

Figure 4 Scanning electron micrographs of CAP glass-ceramic–316 L stainless steel composites: (a) general view of the surface; (b) detailed view of the surface showing thin void spaces (TVS) between matrix and particles.

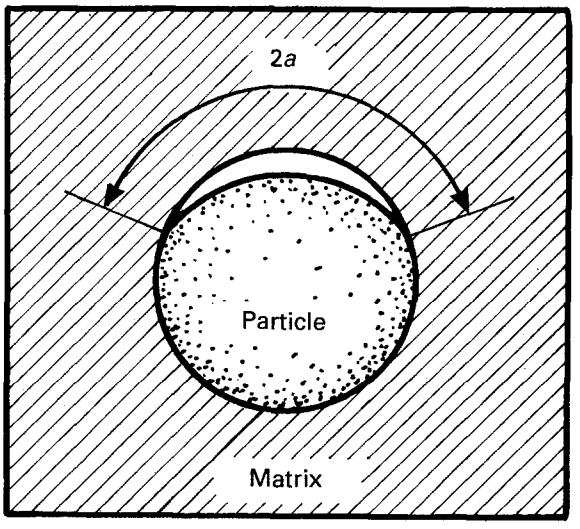

Figure 5 A "spherical segment-shaped flaw" due to partial debonding of a 316 L spherical particle and phosphate glass-ceramic matrix.

Furthermore, the fraction, f, of unbonded surface can be defined as

$$f = \frac{S_{ub}}{S_p} \quad (6)$$

where S_{ub} is the unbonded surface, and S_p is the total

particle surface, with

$$S_{ub} = S_{flaw}$$
$$= \pi a^2 \quad (7a)$$
$$S_p = 4\pi R^2 \quad (7b)$$

so that from Equation 6

$$a = 2Rf^{1/2} \quad (8)$$

Combining Equations 4, 5 and 8 leads to

$$E = E_0\left(1 + \frac{32c_p}{3\pi}f^{3/2}\right)^{-1} \quad (9)$$

Fig. 6 shows that most experimental results lie within two curves drawn for $0.13 \leqslant f \leqslant 0.22$, the best fit being obtained for $f = 0.17$ ($\Delta E/E = 0.8\%$), which means that, on average, more than 80% of the particle surface remains bonded to the matrix.

This result is quite satisfactory in the sense that f does not vary over a very large range for materials which have been obtained using very similar ways; however, in view of the hypotheses assumed for calculations, it must only be considered as a crude approximation. In fact, using other hypotheses, experimental results can be fitted with curves corresponding to fractions of unbonded surface higher than 17%.

Such results are obtained using a model, which gives a method of analysis for the mechanical properties of filler-reinforced elastomers. In such a theory, particles are considered as spherical, rigid and uniformly dispersed in a rubber-like matrix. The one-body approximation is assumed, i.e. particles only prevent more or less matrix from straining, which depends on the state of adhesion between both phases. The actual state of adhesion is approximated by a mixture of two idealized states: one (ideal state I) is the ideal state in which the medium adheres perfectly to the particles, and the other (ideal state II) is the ideal state of perfect non-adhesion in which the medium and the particles exhibit no interaction. With such hypotheses, reinforcement consists of three effects: the volume effect, the surface effect and the cavitation effect [34].

Although metals in glass or glass-ceramic matrix are far from rigid fillers in rubbery media, such a model has already been used to estimate the elastic modulus of glass-matrix composites containing completely decohesed nickel particles [28]. In CAP glass-ceramic–316 L stainless steel system, the elastic modulus of 316 L, 193 GPa, is not higher than three times the elastic modulus of the matrix, 68 GPa; however, the experimental values of elastic moduli of composites, have also been fitted using this model (Fig. 7). Preliminary studies lead us to conclude that particles are at least partly bonded to the matrix, in agreement with the previous interpretation. However, this model gives a "degree of adhesion" [34] significantly lower ($\leqslant 0.6$) than previously ($\geqslant 0.8$) found, and it is only suited to volume fractions not exceeding 30% (Fig. 7). The study of mechanical properties could permit choosing between both interpretations.

3.3. Mechanical properties

Mechanical properties of glass-ceramic–316 L stainless steel composites have been studied as a function of metal volume fraction, c_p (Table II). This table also, gives for each composite, the average distance between particles, d_f, which is taken to be equal to the mean free path [35]

$$d_f = \frac{4R(1 - c_p)}{3c_p} \quad (10)$$

where R is the average radius of particles, and c_p is the volume fraction of inclusions.

Fracture toughness, K_{IC}, and fracture energy, Γ (Fig. 8a and b) increase from 0%–3.5% inclusions; then a discontinuity is observed between 3.5% and 6% inclusion; finally K_{IC}, increases slightly (Fig. 8a), while Γ slightly decreases linearly from 6%–50% (Fig. 8b, full line).

This behaviour could be due to the method of synthesis: for glass-ceramic without any adjuvent, and also for 3.5% 316 L composite, ceramization treatment has been carried out at 700 °C instead of 730 °C for 6%–50% 316 L composites. Both these treatments

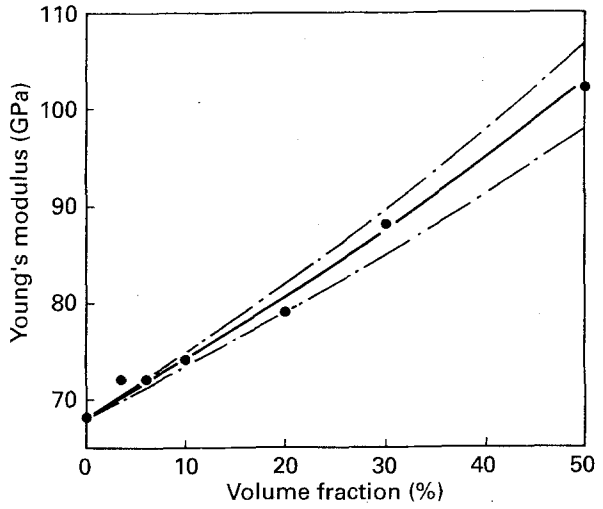

Figure 6 Theoretical (from Equation 9) and experimental Young's modulus of CAP glass-ceramic–316 L stainless steel composites.

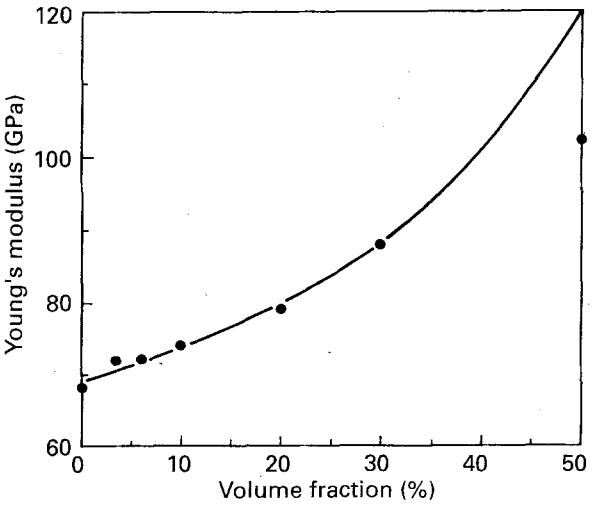

Figure 7 Theoretical (from [34]) and experimental Young's modulus of CAP glass-ceramic–316 L stainless steel composites.

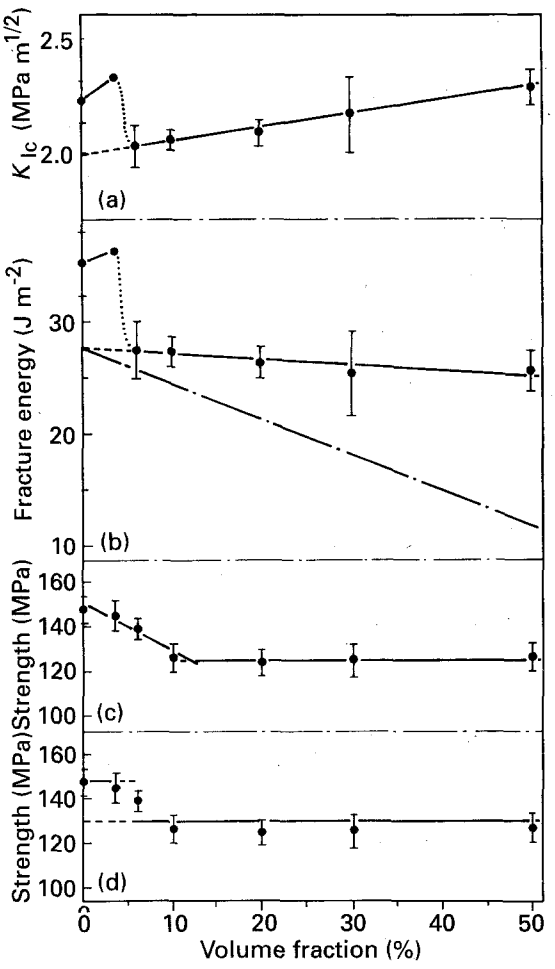

Figure 8 Mechanical properties of CAP glass-ceramic–316 L stainless steel composites: (a) fracture toughness; (b) fracture energy; (c, d) fracture stress.

would induce two evolution ranges with a discontinuity between them. The treatment, performed at higher temperature, could produce an increase of matrix grain size and thus an alteration of its mechanical properties, without changing its Young's modulus [9]. As a result, in 6%–50% 316 L composites, the matrix would have a fracture energy of 27.6 J m^{-2} (instead of 35 J m^{-2} for matrix without any particles) and a toughness of 1.99 MPa m$^{1/2}$ (instead of 2.22 MPa m$^{1/2}$); both values corresponding to extrapolation to zero volume fraction of each experimental straight line (Fig. 8a and b). These 6%–50% 316 L composites thus show a behaviour different from 3.5% 316 L composite, in agreement with results deduced from the first interpretation proposed in the study of elastic properties.

It is also interesting to compare the mechanical behaviour of 6%–50% CAP glass-ceramic–316 L composites to that of CAP glass-ceramic–cobalt–chromium alloy composites. In this last system, where particles are not bonded to the matrix, fracture toughness can be considered as a constant, while fracture energy continuously decreases according to an expression based on typical stereology [6]

$$\Gamma = \Gamma_m(1 - c_p) \quad (11)$$

where Γ_m is the fracture energy of the matrix.

The comparison shows that for 316 L composites: (1) K_{IC} increases instead of being constant; (2) the use of Equation 11, in which Γ_m is taken equal to 27.6 J m^{-2} (fracture energy of "modified matrix"), permits drawing a straight line (Fig. 8b, dotted line), which shows a steeper decrease than the experimental curve (Fig. 8b, full line).

All these results tend to prove that particles are at least partly bonded to glass-ceramic matrix, in agreement with results deduced from elastic property study. In the case of fracture energy, the difference between experimental values (Fig. 8b, full line) and those deduced from the theoretical straight line (Fig. 8b, dotted line) could be due both to the decohesion of weakly bonded particles, creating "pseudopores", and also to local blunting, when the crack front intersects newly formed pseudopores [31].

The results of strength measurements cannot be explained so easily as those deduced from the study of other mechanical properties; two interpretations can be proposed. The first one considers two evolution regions: 0%–10% 316 L then 20%–50% 316 L.

Between 0% to just above 10% inclusions, fracture stress, σ_R, of 316 L composites would show a monotonic linear decrease, from the strength of the matrix, σ_{Rm}, (Fig. 8c) according to

$$\sigma_R = \sigma_{Rm}(1 - \alpha c_p) \quad (12)$$

This equation means that: (1) the system would behave as being "pseudo-porous": particles do not contribute to the strength of materials and c_p is thus a pore volume fraction; (2) the pseudo-pore size (i.e. the size of 316 L particles) would be small relative to the flaw size, a_c, [27], which is actually obtained because these sizes are, respectively, $\approx 10\,\mu m$ and $\geqslant 55\,\mu m$, assuming a Griffith flaw, or $\geqslant 132\,\mu m$, assuming a penny-shaped crack. Moreover, the constant, α, of Equation 12 (≈ 1.4) deduced from Fig. 8c is slightly lower than the value (1.5) calculated theoretically for spherical pores [36], which could be due to the irregular shape of most 316 L particles.

Between 20% and 50% inclusions, σ_R would remain practically constant (Fig. 8c), which is more difficult to explain in this context. In this volume percentage range, the decrease of interparticle spacing with respect to critical flaw size (Table II) could induce interactions between the stress field around pseudo-pores and the stress distributions around the flaw and thus explain another variation law of σ_R versus c_p.

In this first interpretation, the two evolution ranges (0%–10% and 20%–50%) do not correspond to those observed previously (0%–3.5% and 6%–50%). Assuming a continuous decrease of σ_R within the region 0%–10% 316 L, a difference between the behaviour of 3.5% 316 L composite and that of the others is no longer seen. Moreover, the constancy of σ_R just above 10% cannot be very clearly explained.

Another interpretation would then consist of assuming that ceramization at 730 °C and resulting increase of grain size also alters the strength of the matrix in 6%–50% 316 L composites, as was observed for toughness and fracture energy. The

"modified" matrix would have a fracture stress, σ'_{Rm}, of about 130 MPa (Fig. 8d). The partial bond between matrix and particles would then explain why, in a first approximation, strength, σ_R, does not show a significant variation from 6%–50% inclusions instead of decreasing as in a "true pseudoporous" system [28, 36]. This new interpretation is more consistent with those deduced from the study of elastic modulus, fracture toughness and fracture energy, although strength of the 6% 316 L composite is rather high.

4. Conclusion

Glass-ceramic–316 L stainless steel composites could be obtained from mixtures of a calcium aluminophosphate parent glass (CAP) and various volume fractions (up to 50%) of 316 L stainless steel particles. They have been prepared by hot-pressing using the "flash pressing" technique.

The elastic moduli of 6%–50% 316 L composites, measured by dynamic methods, have been found just above Reuss's curve [20] but below theoretical values assumed to correspond to the average between upper and lower bound of Hashin and Shtrikman's model [21]. This has led us to conclude that particles were only partly bonded to the matrix in these 6%–50% composites. From the departure between theoretical and experimental values of elastic modulus, a fraction of the remaining bonded surface has been estimated to be about 80%.

This precise value could not be confirmed by the study of mechanical properties; however, this last study also showed that particles were at least partly bonded to the matrix. Owing to differences in preparation method, the matrix of 6%–50% 316 L composites have been found to have mechanical properties, different from those of the matrix without any adjuvent.

A model, which gives a method of analysis for the mechanical properties of filler-reinforced elastomers, has been also used to estimate the elastic modulus of CAP glass-ceramic–316 L stainless steel composites. Preliminary results have also led us to conclude that particles were partly bonded to the matrix, with a "degree of adhesion" lower than 60%; however, this model has given satisfactory fits, only for composites with particle volume fractions not higher than 30%. The study of all the mechanical properties has not shown significant differences of the 50% 316 L composite with respect to the behaviour of composites with lower particle volume fractions. As a result this model does not appear, at the present time, as suitable to improve the interpretations significantly.

References

1. I. W. DONALD and P. W. McMILLAN, *J. Mater. Sci.* **11** (1976) 949.
2. J. J. MECHOLSKY, *Am. Ceram. Soc. Bull.* **65** (1986) 315.
3. R. ROGIER and F. PERNOT, *J. Mater. Sci. Mater. Med.* **2** (1991) 153.
4. F. PERNOT, J. ZARZYCKI, F. BONNEL, P. RABISCHONG and P. BALDET, *J. Mater. Sci.* **14** (1979) 1694.
5. R. ROGIER and F. PERNOT, *ibid.* **26** (1991) 5664.
6. F. PERNOT and R. ROGIER, *ibid.* **27** (1992) 2914.
7. B. R. JENNINGS and K. PARSLOW, *Proc. R. Soc. Lond.* **A419** (1988) 137.
8. M. DECOTTIGNIES, J. PHALIPPOU and J. ZARZYCKI, *J. Mater. Sci.* **13** (1978) 2605.
9. R. W. RICE, in "Treatise on materials Science and Technology", Vol. 11, edited by R. K. MacCrone (Academic Press, New York, 1977) p. 199.
10. W. F. BROWN and J. E. SRAWLEY, ASTM Special Technical Publication 410, Baltimore (1967) p. 1.
11. A. G. EVANS and G. TAPPIN, *Proc. Br. Ceram. Soc.* **23** (1972) 275.
12. J. L. CHERMANT and F. OSTERSTOCK, *J. Mater. Sci.* **11** (1976) 1939.
13. A. J. LEADBETTER and T. W. SMITH, *Philos. Mag.* **33** (1976) 105.
14. W. F. HORN and F. A. HUMMEL, *J. Am. Ceram. Soc.* **63** (1980) 338.
15. P. S. TURNER, *J. Res. Nat. Bur. Stand.* **37** (1946) 239.
16. S. J. FELTHAM, B. YATES and R. J. MARTIN, *J. Mater. Sci.* **17** (1982) 2309.
17. E. H. KERNER, *Proc. Phys. Soc.* **B69** (1956) 808.
18. F. F. LANGE, in "Composites Materials", Vol. 5, edited by L. J. Broutman (Academic Press, New York, 1974), p. 1.
19. W. VOIGT, "Lehrbuch der Kristallophysik" (Teubner, Berlin, 1910).
20. W. REUSS, *Z. Angew. Math. Mech.* **9** (1929) 49.
21. Z. HASHIN and S. SHTRIKMAN, *J. Mech. Phys. Solids* **11** (1963) 127.
22. J. SELSING, *J. Am. Ceram. Soc.* **44** (1961) 419.
23. R. W. DAVIDGE and T. J. GREEN, *J. Mater. Sci.* **3** (1968) 629.
24. D. B. BINNS, in "Science of Ceramics", Vol. 1, edited by G. H. Stewart (Academic Press, New York, 1962) p. 315.
25. F. F. LANGE, in "Fracture mechanics of ceramics", Vol. 2, edited by R. C. Bradt, D. P. H. Hasselman and F. F. Lange (Plenum Press, New York, 1974) p. 599.
26. D. J. GREEN, *J. Am. Ceram. Soc.* **64** (1981) 138.
27. D. P. H. HASSELMAN and R. M. FULRATH, *ibid.* **45** (1962) 592.
28. D. J. GREEN, P. S. NICHOLSON and J. D. EMBURY, *J. Mater. Sci.* **14** (1979) 1413.
29. J. A. PASK and R. M. FULRATH, *J. Am. Ceram. Soc.* **45** (1962) 592.
30. M. A. STETT and R. M. FULRATH, *ibid.* **53** (1970) 5.
31. A. K. KHAUND and P. NICHOLSON, *J. Mater. Sci.* **15** (1980) 177.
32. D. P. H. HASSELMAN and J. P. SINGH, *Am. Ceram. Soc. Bull.* **50** (1977) 559.
33. D. J. GREEN, *J. Am. Ceram. Soc.* **65** (1982) 610.
34. Y. SATO and J. FURUKAWA, *Rubber Chem. Technol.* **36** (1963) 1081.
35. R. L. FULLMAN, *Trans. AIME J. Met.* **197** (1953) 447.
36. S. D. BROWN, R. B. BIDDULPH and P. WILCOX, *J. Am. Ceram. Soc.* **47** (1964) 320.

Received 17 November 1992
and accepted 29 April 1993